Available online at www.sciencedirect.com
ScienceDirect
Trans. Nonferrous Met. Soc. China 35(2025) 3108−3119
Transactions of Nonferrous Metals Society of China
www.tnmsc.cn

Metallogenic environment in central southern Tanlu Fault revealed by P-wave tomography

Ya SUN[1], Zi-jun YUAN[1], Ji-wen HUANG[1], Jian-tai ZHANG[2], Fu-quan LI[2], Jian-xin LIU[1]

1. School of Geosciences and Info-Physics, Central South University, Changsha 410083, China;
2. No. 7 Geological Team of Shandong Provincial Bureau of Geology Mineral Resources, Linyi 276000, China

Received 10 January 2024; accepted 30 September 2024

Abstract: A P-wave velocity model was built in the central southern of the Tanlu Fault based on double-difference tomography. The results suggest the presence of a low-velocity anomaly extending from the surface to a depth of 25 km around the Tanlu and Feixi Faults, representing fault-related fluids caused by partial melting. The relocated earthquakes indicate a significant concentration of seismic activity above 20 km around the Tanlu and Feixi Faults, suggesting that prominent fault systems possibly serve as conduits for the upward migration of deep minerals. The proposed geodynamic model, supported by geological and geophysical data, suggests that the migration of deep mineralized materials extends along the Tanlu Fault. The obtained results serve as a crucial foundation for elucidating the intricate process of mineralization in the central southern segment of the Tanlu Fault, thereby enhancing comprehension regarding the interaction among ore body formation, fault fluids, localized melting, and seismic activity.

Key words: central southern Tanlu Fault; double-difference tomography; mineralization; partial melting; P-wave velocity

1 Introduction

The Tanlu Fault, a prominent and active fault in eastern China, exhibits a north−south orientation and extends across provinces including Anhui, Jiangsu, Shandong, and Heilongjiang (Fig. 1(a)). The Tanlu Fault, being the most dynamic and extensive fault in the region, has garnered significant attention as the primary seismic tectonic zone [1]. It comprises a primary fault and a series of subsidiary faults that have caused significant crustal deformation and generated large earthquakes in the region [2]. The Tanlu Fault exhibits a complex geometry and can be categorized into northern, central, and southern segments based on the characteristics of the aeromagnetic measurements, gravity, geological structure, magmatic activity, and seismic activity [3]. This study focuses on the central−south region of the Tanlu Fault (114°E−120°E, 30°N−38°N) shown in Fig. 1(b), encompassing Shandong, Anhui, and Jiangsu Provinces.

The Tanlu Fault is significant in mineral resources, including gold, copper, and iron (Fig. 2) [4]. Geochemical studies indicated that the mineral deposits are associated with magmatic rocks [5]. Multiple Early Cretaceous dioritic intrusions exhibit prominent high-Mg adakitic geochemical characteristics in the central southern Tanlu Fault [4,5]. The intrusions of high-Mg adakites are considered to have formed as a result of partial melting of an over-thickened basaltic lower crust following the delamination of the eclogitic lithosphere during the Late Jurassic to Early Cretaceous [5]. Receiver functions along the Tanlu

Corresponding author: Jian-xin LIU, Tel: +86-13807486248, E-mail: ljx@csu.edu.cn
https://doi.org/10.1016/S1003-6326(25)66869-5

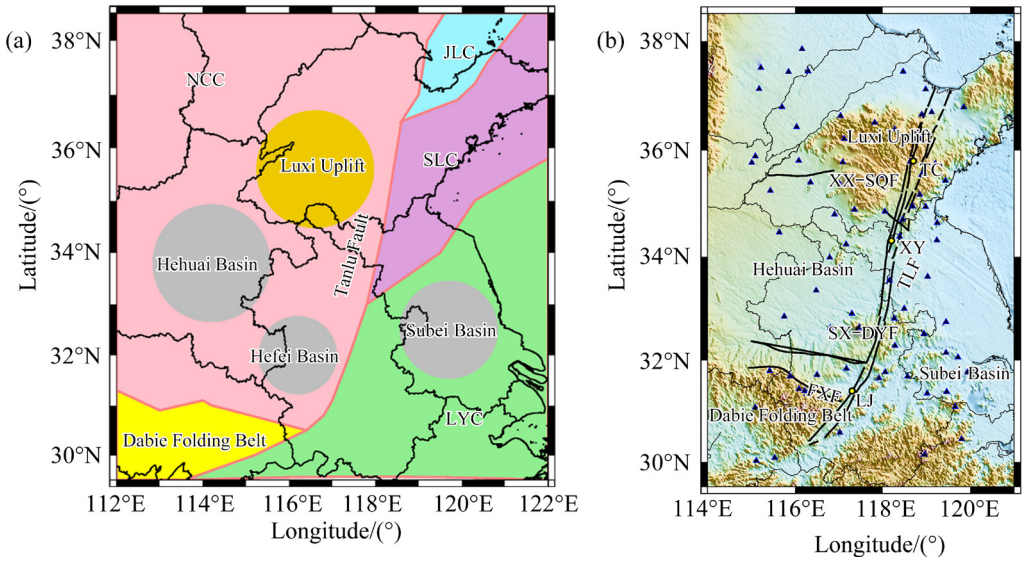

Fig. 1 Tectonic blocks (a) [1] and distribution of seismic stations (blue triangles) (b) (NCC: North China Craton; SLC: Sulu Craton; JLC: Jiaoliao Craton; LYC: Lower Yangtze Craton; TLF: Tanlu Fault; XX—SQF: Xinxiang—Shangqiu Fault; SX—DYF: Shouxian—Dingyuan Fault; FXF: Feixi Fault; LJ: Lujiang; XY: Xinyi; TC: Tancheng earthquake)

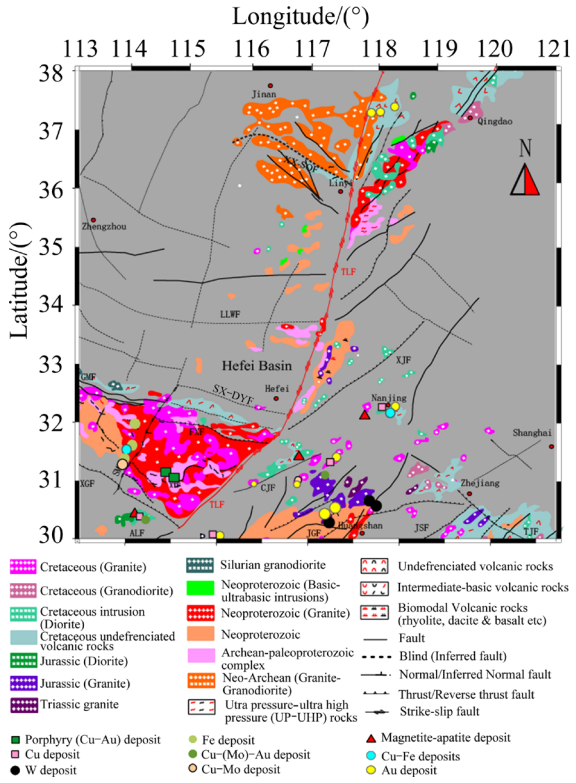

Fig. 2 Geological and metallic mineral deposits in eastern China (TLF: Tanlu Fault; LLWF: Lingbo—Lushan—Wuyang Fault; GMF: Guishan—Meishan Fault; ALF: Anhua — Luocheng Fault; XTF: Xishui — Tongcheng Fault; XGF: Xiangfan—Guangji Fault; CJF: Changjiang Fault; JSF: Jiangshan—Shaoxing Fault; TJF: Turong—Jianyang Fault; JGF: Jiangnan Fault; FXF: Feixi Fault and ZDF: Zhenghe—Dapu Fault [7])

Fault indicate that the lithosphere has thinned significantly since the Paleozoic, decreasing from an initial thickness of 180 km to 60−80 km [6]. Does the formation of minerals on the Earth's surface result from the lithosphere thinning and upwelling of hot material along the Tanlu Fault? The correlation between the ore-forming environment and fault activity in the region, as well as the deep dynamic process, has been a hot topic.

The activity of faults and the formation process of minerals on the Earth's surface are accompanied by variations in seismic wave velocity within the crust. Due to the complexity and significance of geological and tectonic evolution in the research region, numerous seismic images have been used to explain the formation and evolution of the fault, seismic activity, and the geodynamic mechanisms underlying deep mineralization [6−11]. Deep seismic reflection profiles demonstrate that a series of interconnected segments vary in width and depth of the Tanlu Fault, which suggests that several segments have complex structures with multiple fault strands [6]. A significant anomaly with a high Poisson's ratio is observed along the Tanlu Fault in the NNE−SSW direction based on receiver function data [12,13]. It is hypothesized that the increase in Poisson's ratio can be attributed to either the infiltration of mafic magma through the weak structure of Tanlu Fault into the crust or the rapid attenuation of S-waves caused by the

intrusion of high-temperature and high-pressure thermal materials from mantle upwelling [12,13]. The geophysical data served as a crucial foundation for further comprehending the formation and evolution of the Tanlu Fault [11−15]. The refined crustal structure provides significant implications for further understanding the correlation between the seismic activity and the deep mineralized environment in the region.

Both absolute and differential arrival time were utilized for earthquake relocation and seismic wave velocity inversion using the double-difference seismic tomography method. Differential arrival times, in particular, enhance the efficiency of determining source velocity structures. This technology has proven to be effective in studying the geodynamics of deep mineralization and examining the correlation between seismic relocation and fault matching [16]. The double-difference seismic tomography method was employed to relocate earthquakes and invert the crustal structure based on the first P-wave data from 3353 seismic events recorded at 84 stations by the China Earthquake Administration (CEA) network between 2009 and 2020. These results contribute significantly to a comprehensive understanding of the evolution, activity, and dynamic mechanisms of the fault system related to deep mineralization.

2 Geological setting

The tectonic evolution of Eastern China is shaped by the interaction of multiple cratons and orogenic belts, including the Yangtze Craton, North China Craton, Sulu Orogen, Dabie Orogenic Belt, and Tanlu Fault [2]. The Yangtze Craton, one of the oldest and most stable cratons in the world, was formed during the Archean period [15]. The North China Craton, another ancient craton, originated during the Proterozoic period [17]. These two cratons collided during the Mesozoic era, leading to the formation of the Sulu Orogenic Belt [18,19], which has obviously affected the tectonic evolution of Eastern China. The Sulu Orogenic Belt, located on the eastern edge of the North China Craton, is characterized by high-quality metamorphic rocks, magmatic rocks and granitic gneisses [20]. Its formation is attributed to the collision and compression of the North China Craton and the Yangtze Craton [21].

The research region had experienced multiple magmatic episodes, resulting in the formation of various igneous rocks [20]. The magmatic episodes were primarily associated with tectonic events (Fig. 2), including the collision of the Yangtze and North China Cratons and the subduction of the Pacific Plate [7]. The magmatic rocks in Eastern China are grouped into two significant types: plutonic rocks and volcanic rocks [22]. The plutonic rocks include granitic rocks and granodiorites, which are common in the Qinling—Dabie Orogenic Belt and the Sulu Orogen [23]. The volcanic rocks include basalts, andesites, and rhyolites, which are widely distributed in the Tanlu Fault and other regions of Eastern China. Previous studies [23,24] suggested that the ore formation in this research area is controlled by partial melting of fertile metasedimentary rocks.

3 Data and methods

3.1 Data

The research area is situated in the central southern segment of the Tanlu Fault, covering parts of both the North China Craton and the Lower Yangtze Craton, in the range of 114°E−120°E and 30°N−38°N (Fig. 1(b)). The first P-wave arrival time data were collected from 3353 seismic events recorded at 84 stations by the CEA network between 2009 and 2020 (https://data.earthquake.cn). To ensure reliability, phase data with uncertainties smaller than ±9 s relative to the predominant trend of the travel time curves for P-waves were selected (Fig. 3). The arrival time data were subsequently refined, requiring a minimum of 8 stations to record seismic events. Seismic events were then reduced from 3353 to 2752, with a magnitude greater than 1.0. The total of 201068 initial P-wave arrivals are recorded of which 130445 differential arrivals are selected for further analysis. The high-quality ray coverage provided by the combination of all P-wave arrivals and event pairs enhances the reliability of double-difference tomography.

3.2 Method

According to the ray theory, the arrival time (T_k^i) from event i to station k can be represented as

$$T_k^i = \tau^i + \int_i^k u \mathrm{d}s \tag{1}$$

where τ^i and u represent the origin time and the

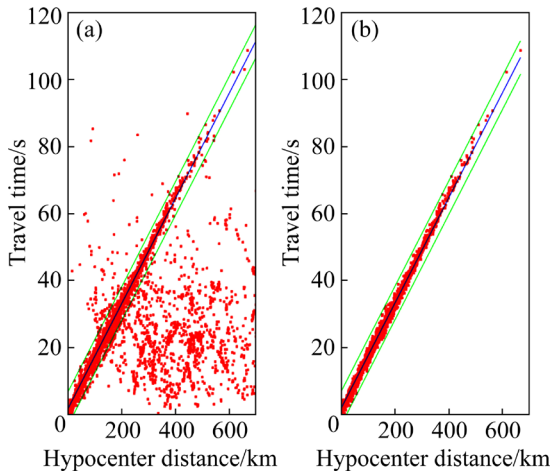

Fig. 3 Travel time−hypocenter distance curves of P-wave before (a) and after (b) filtering

slowness of event i, respectively; ds is the ray path segment length. Taylor series expansion of Eq. (1) can be written as

$$r_k^i=\sum_{l=1}^{3}\frac{\partial T_k^i}{\partial x_j^i}\Delta x_j^i+\Delta\tau^i+\sum_{m=1}^{M_{ik}}\sum_{n=1}^{N}w_{mn}\Delta u_n\Delta s_m \tag{2}$$

where r_k^i is the residual between the observed and theoretical travel time; Δx (l=1, 2, 3) and Δu are the perturbations of the source location and the slowness, respectively; $\Delta\tau$ is the perturbation of arrival time; M_{ik} denotes the count of the ray path segments between event i and station k. The weight w_{mn} represents the interpolating value of the nth mesh node at the mid-point of the mth segment with a length of ΔS_m. We choose a pair of events i and j observed at the same seismic station k. The residual time of a pair of events can be expressed as [25,26]

$$r_k^i-r_k^j=\sum_{l=1}^{3}\frac{\partial T_k^i}{\partial x_l^i}\Delta x_l^i+\Delta\tau^i+\sum_{m=1}^{M_{ik}}\sum_{n=1}^{N}w_{mn}\Delta u_n\Delta s_m-$$
$$\sum_{l=1}^{3}\frac{\partial T_k^i}{\partial x_l^j}\Delta x_l^j-\Delta\tau^j-\sum_{m=1}^{M_{jk}}\sum_{n=1}^{N}w_{mn}\Delta u_n\Delta s_m=\mathrm{d}r_k^{ij} \tag{3}$$

where $r_k^i-r_k^j$ is the double-difference term [26,27]. It refers to the residual time between the observed and calculated arrival time for the two events, and can also be expressed as [26]

$$r_k^i-r_k^j=(T_k^i-T_k^j)^{\mathrm{obs}}-(T_k^i-T_k^j)^{\mathrm{cal}} \tag{4}$$

Equation (4) is a pair of seismic events i and j at the same station k. We set the maximum and minimum distance for event pairs to be 300 and 10 km, respectively. Combining the relationship of all seismic events (i, j=1, 2, 3, ⋯, N) and all stations (k=1, 2, 3, ⋯), the seismic position, seismic time and seismic wave velocity can be obtained by solving the equation. The three-dimensional velocity structure and seismic relocation are inverted based on absolute time and relative data. Absolute data are used to determine the velocity structure outside the source region, while relative data are employed to determine the fine velocity structure within the source area. The integration of absolute and differential data is achieved by implementing a hierarchical weighting scheme during the inversion process, which effectively assigns appropriate relative weights at different stages. Initially, utmost priority is given to catalog data (both differential and absolute) by applying higher weighting to establish the macroscopic velocity structure (1 for absolute data, and 0.1 for differential catalog data). The weight assigned to differential data is 1, while the weight assigned to absolute data in the later iterations is reduced to 0.1 [26]. The adjustment effectively constrains the velocity structure near the source area and enhances the accuracy of event locations. The solution is then obtained by solving the regular equation using the damped least squares method. We choose the L-curve method to determine the damping and smoothing factors for inversion (Fig. 4). The smoothing and damping factors are selected as 10 and 400, respectively.

The one-dimensional (1D) P-wave velocity is chosen as the initial model to invert the crustal structure. The version results are reasonable with the 1D initial model. The 3D P-wave velocity is also used as the initial model with a grid interval of 0.5°, which is calculated by the empirical formula of v_P (v_P is the velocity of P-wave) and v_S (v_S is the velocity of S-wave) [28] based on the 3D crustal v_S model inverted by ambient noise tomography [22]. The inversion results can better display detailed structures compared to the inversion results based on the 1D initial model, especially in the Tanlu Fault and Dabie Orogenic Belt. Finally, a 3D v_p initial model is chosen, and the vertical grid notes are at −5, 0, 3, 5, 10, 15, 20, 25, and 30 km, respectively.

3.3 Checkerboard resolution test

The checkerboard resolution test was used to

evaluate the resolution of velocity models under the current ray path coverage. The input model includes the 5% low- and high-velocity anomalies, with an anomaly size of 0.5° × 0.5°. The synthetic travel time is then calculated with the same distribution of events and stations as accurate data. The checkerboard test results are shown in Fig. 5, which suggests that it is recovered at depths from 0 to 30 km in the research region with high-quality data coverage.

4 Results

4.1 Earthquake relocations

2276 seismic events are relocated after 10 iterations using the double-difference tomography method. Figure 6 demonstrates that the relocated earthquakes are mainly distributed along the fault strike, especially at the Feixi and Tanlu Faults. The average root mean square of travel time residuals after inversion significantly decreases relative to that before relocation. The travel time residuals vary from −3 to 3 s before relocation, with a predominant concentration within 1 s. However, the travel time residuals exhibit a significant concentration within 0.2 s after relocation (Fig. 7), indicating a substantial enhancement in the accuracy of earthquake relocation by the double-difference technique.

4.2 Crustal velocity structure

The inverted seismic velocity model (Fig. 8) shows that the southern segment of the Tanlu Fault is mainly characterized by low-velocity anomalies

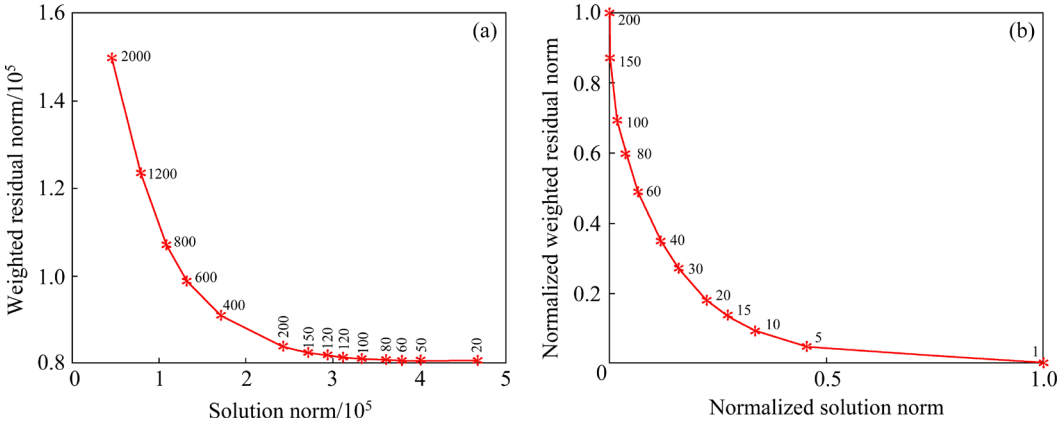

Fig. 4 Tradeoff curves between data residual norm and solution norm for damping parameter (a) and smoothing parameter (b)

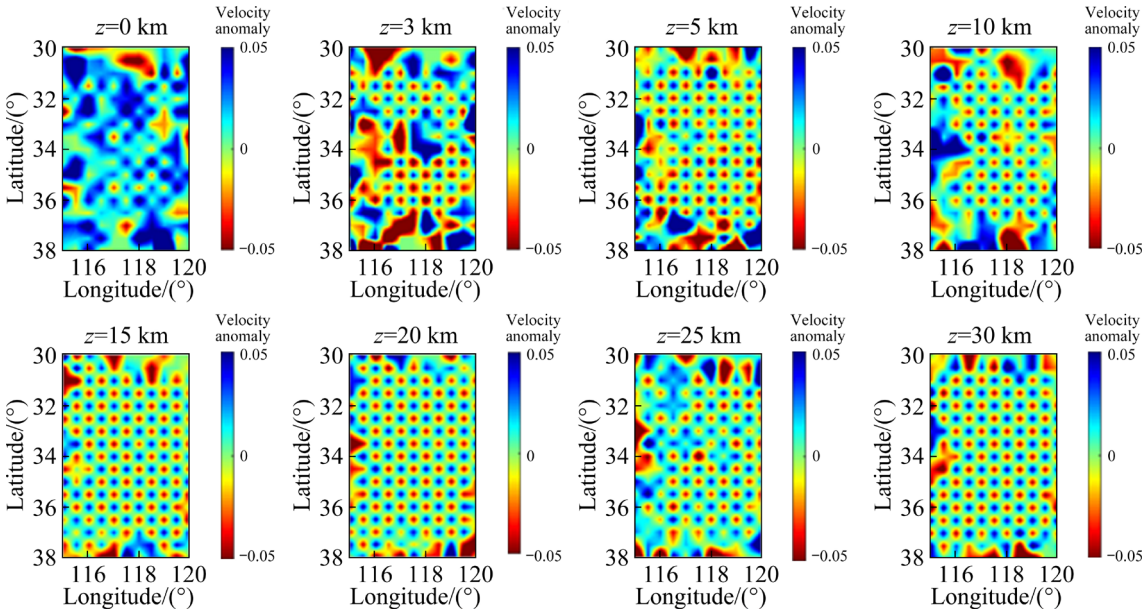

Fig. 5 Recovered checkerboard patterns for P-wave velocity at depths (*z*) of 0, 3, 5, 10, 15, 20, 25, and 30 km

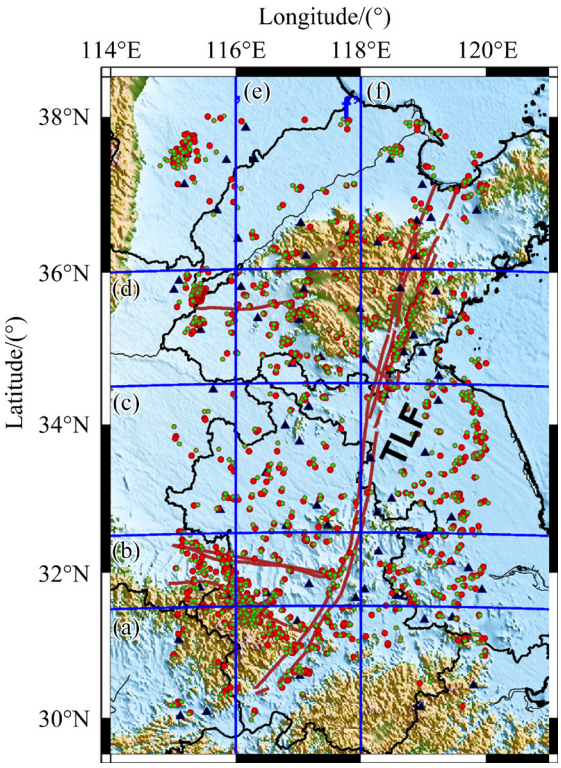

Fig. 6 Distribution of seismic events before (red circles) and after (green circles) double-difference relocation

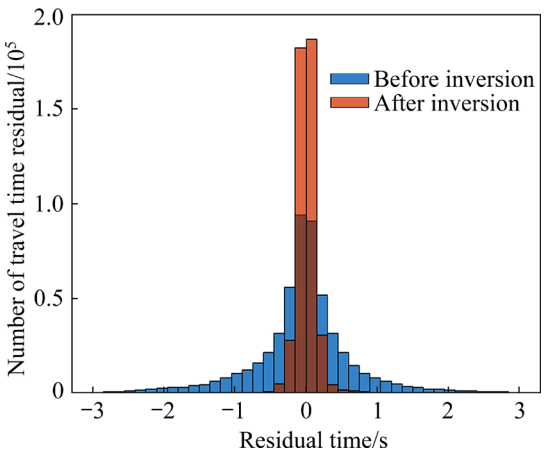

Fig. 7 Histogram of travel time residuals before and after inversion

in the upper crust (<10 km). A significant high-velocity anomaly is imaged in the Luxi Uplift from depths of 10 to 28 km. The high-velocity anomaly exhibits a gradual northward inclination with increasing depth (Fig. 8). The Subei Basin in the upper crust exhibits a low-velocity anomaly, accompanied by high-velocity anomalies in the lower crust. The findings indicate that the low-velocity anomaly in the Dabie Folding Belt extends southward within the upper crust. The Dabie Folding Belt and its northern region exhibit a high-velocity anomaly in the upper crust and low-velocity anomaly in the middle and lower crust. The research results also show the obvious low-velocity anomaly in the upper crust in the Hehuai, Hefei, and Subei Basins, while the relatively high-velocity anomaly in the middle and lower crust in these basins (Fig. 8).

Six vertical profiles of P-wave velocity are also plotted with the distribution of earthquakes in Fig. 9. The vertical profiles exhibit a distinct low-velocity anomaly within the depth range of 0−25 km beneath the Tanlu Fault, while conspicuous high-velocity anomalies are observed on both flanks of the Tanlu Fault. The low average velocity of P-wave is 3.5−4.5 km/s in the range of 115.5°E to 116.3°E along 31.5°N and 32.5°N beneath the Tanlu Fault (Figs. 9(a, b, d, e, f)), implying that the crustal materials in the research region have relatively low density, high porosity, or high fluid content. The presence of low-velocity anomalies can be attributed to a variety of geological processes, including fracturing, weathering, metamorphism, or magmatism. The vertical profiles suggest that there are nearly vertical low-velocity anomalies from the surface to the middle and lower crust or even to the uppermost mantle in both the Feixi Fault and Tanlu Fault, accompanied by many seismic events (Fig. 9). The relatively high P-wave velocity features are obvious performance in the Luxi Uplift, Subei, and Hehuai Basins in the middle and lower crust, whereas the low velocities are present in the upper crust. The high velocity might be attributed to the rigid stable blocks in the Luxi Uplift, Subei, and Hehuai Basins, while the low velocity in the upper crust is relative to the thick sedimentary layers.

5 Discussion

5.1 Mechanism of high- and ultrahigh-pressure metamorphic rocks in Dabie Orogenic Belt

The results of the research study indicate the presence of a relatively high velocity, ranging from 5 to 6.2 km/s above 12 km in the upper crust beneath the Dabie Orogenic Belt, which is located specifically in the range of 115.5°E−117°E and 30.5°N−31.8°N (Figs. 9(a, b)). The shallow high P-velocity anomalies (Figs. 9(a, b, e)) are consistent with the results of ambient noise tomography that

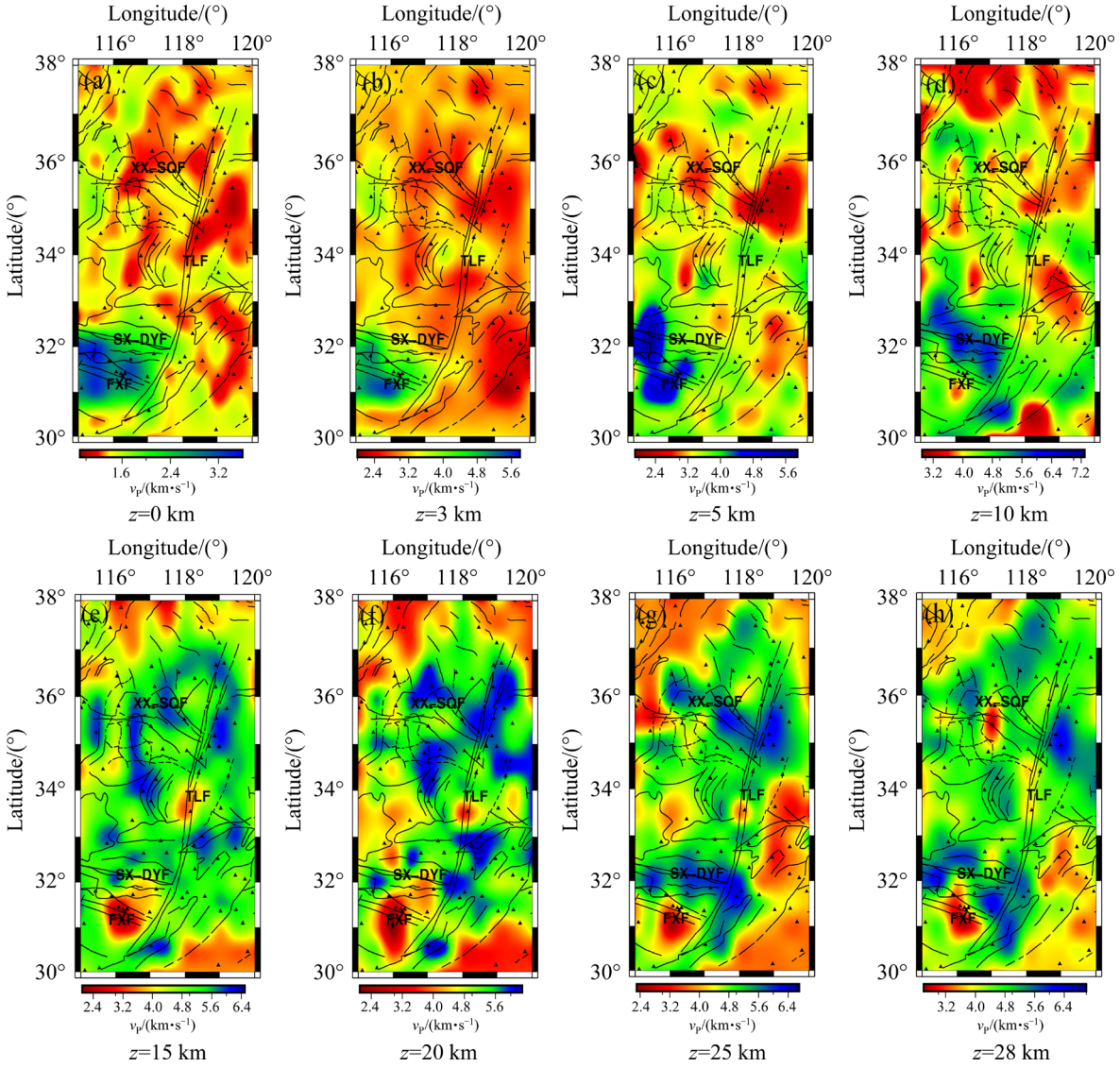

Fig. 8 Horizontal slices of P-wave velocity model at depths of 0, 3, 5, 10, 15, 20, 25, and 28 km

showed the high shear wave velocities in the crust of the Dabie Orogenic Belt [29], which are coincident with the areas where the high- and ultrahigh-pressure (HP/UHP) metamorphic rocks (Fig. 2) are exposed on the surface. These findings are consistent with previous results from deep seismic refraction profiling studies [29,30]. The laboratory data indicate that HP/UHP metamorphic rocks generally demonstrate higher seismic velocities in comparison to other upper crustal rocks [31]. The observed high velocities in the upper crust indicate that HP/UHP metamorphic rocks primarily concentrate within the upper crust.

A distinct low-velocity region in the middle and lower crust, which underlies the high-velocity HP/UHP metamorphic zones, is also observed (Figs. 9(a, b, e)). The research results also indicate that an obvious continuous high-velocity anomaly extends from the east to the west in the Tanlu Fault; it also exhibits a trend of further subduction below the low-velocity anomaly at the Dabie Orogenic Belt (Figs. 9(a, b, e)). Ambient noise tomography indicated that the high-velocity HP/HUP metamorphic rocks in the upper crust could be attributed to a two-stage exhumation model controlled by buoyancy and corner flow [28]. At the beginning of the Triassic period, a collision occurred between the Yangtze Craton and the North China Craton, resulting in the subduction of the Yangtze Craton towards the North China Block. The presence of a high-velocity anomaly on the eastern side of the Tanlu Fault signifies the subducted Yangtze Craton. During continental collision, crustal rocks are entrained by the subducting Yangtze Craton,

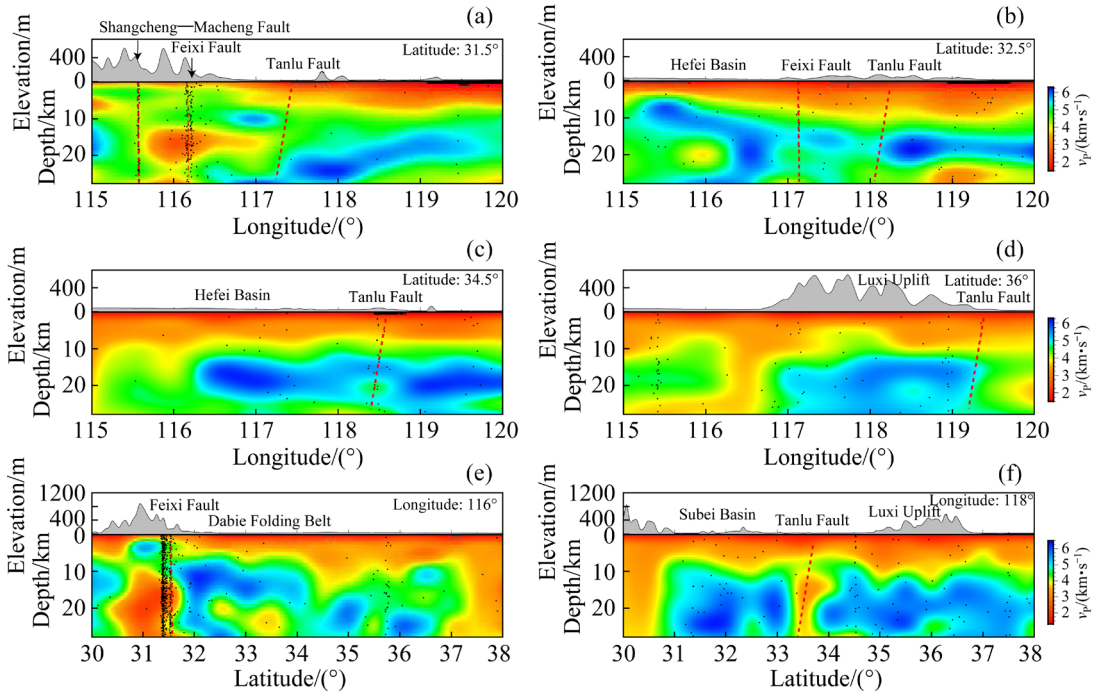

Fig. 9 Vertical sections of P-wave velocity model along profiles shown in Fig. 6 (The black points represent the earthquakes, and the red dashed lines represent the faults)

descending into the upper mantle, and HP/UHP metamorphism rocks occur under high temperatures and high pressure [32]. Due to the lower density of crustal rocks compared to mantle rocks, the HP/UHP material from deep subduction ascends obliquely along the subduction channel towards the crust. The HP/UHP metamorphic rocks are ultimately brought to the Earth's surface due to the continuous compression of the Pacific Plate and deep subduction of the Yangtze Craton [33]. The presence of low velocities beneath high velocity beneath the Dabie Orogenic Belt can be attributed to the development of ductile shear zones or brittle fracture zones during the exhumation process of these metamorphic rocks [34].

5.2 Mechanisms of mineral deposits formation in Tanlu Fault

The observed seismic wave velocity of the crust can provide valuable insights into the geometry and extent of the fault system. The seismic tomography indicates that the prominent low-velocity anomalies are distributed extensively along the Tanlu and Feixi Faults (Figs. 9(a, b, d, e, f), extending down to the middle and lower crust, which are accompanied by a significant concentration of seismic activity. The observed phenomenon indicates the depth and breadth of the two fault zones, potentially extending to the middle and lower crust or even reaching the uppermost mantle. The presence of low-velocity anomalies beneath the Tanlu and Feixi Faults, with an average P-wave velocity of 3.5−4.5 km/s (Figs. 9(a, b, d, e, f), also indicates that the materials in these two faults have a low density with high porosity or high fluid content. The finding is consistent with the previous studies that have similar low P-velocity anomalies observed by the body wave tomography [8,14,35] and low shear wave velocity measured by ambient noise tomography in the region [9,36−38]. Geophysical studies and geological data have revealed the structure complexity of the Tanlu Fault, where deep faults exhibit a variety of orientations and faulting mechanisms [17,22,37]. It is recognized as a significant active fault characterized by extensive fracturing and faulting, which results in the accumulation of fluids within the Earth's crust (Fig. 9(f)) [38−40]. These fluids can be trapped in the pore spaces of rocks or along the fault channel, causing low velocity [38]. Receiver function analysis shows that the crust has significant variations in thin crustal thickness on the eastern side of the boundary between the Jiangsu Province and Anhui Province and a high v_P/v_S ratio

beneath the central−southern segments of the Tanlu Fault [6,12,13,39]. The thin crust and high v_P/v_S ratio observed in the eastern section of the Tanlu Fault could be the result of the lithospheric modification extending into the lower crust, driven by the upwelling of mantle magma via deep crustal faults during the Mesozoic to Cenozoic [39].

The seismic wave velocity may be related to the rock composition in lithology or mineralogy at depth. For example, the transition from sedimentary rocks to metamorphic rocks could increase the velocity [40]. The vertical profiles reveal a clear boundary of high and low velocities at a depth of 10 km (Figs. 9(b, c, d, f)). It has the possibility of being a metamorphic boundary in the crust [40], which could represent a change in the temperature or pressure conditions, leading to the formation of metamorphic minerals. Geological data indicate that crystalline materials are widely distributed in the region [33]. The presence of such material in the region suggests that it can be related to the solidification of a magma system in the middle to lower crust. As magma cools and solidifies, it can form crystalline structures, leading to dense and hard rock formation. This indicates that the observed high P-wave velocity in the lower crust might be caused by the crystalline material, which is attributed to a magma system solidified in the middle to lower crust. The active metamorphism in the region can be attributed to the subduction of the Yangtze Craton and the continuous compression of the Pacific Plate, which has resulted in significant deformation of the rocks in the region, leading to the formation of new structures and mineral assemblages (Fig. 2).

Furthermore, the Tanlu Fault in Eastern China experienced several large earthquakes in the 20th century (Fig. 6), indicating the Tanlu Fault underwent complex deformation and strain accumulation within the crust. Studies of the fault have revealed that the quartz hugely influences the rheology of the rocks in the lower crust during the alpha-to-beta transition [41]. The transition can potentially cause significant alteration in the stress and strain of the rocks, particularly when partial melting occurs [41]. The partial melting of lower crustal rocks can also lead to the formation of new minerals, changes in mineral assemblages, and deformation of the rocks. The alpha-to-beta transition of quartz can contribute to the process by creating a more ductile environment and promoting the grain growth [41]. The transition can result in the formation of schists, gneisses, and other metamorphic rocks, which are abundantly found in the eastern section of the Tanlu Fault [41] (Fig. 2). The rheological properties of crustal rocks can also cause changes in the fluid content of rocks under the alpha-beta transition [41]. It can be inferred that the partial melting and the alpha-to-beta transition can cause changes in the connectivity and mobility of the fluid phases, which can affect the strength and deformation of the rocks [42]. The results also indicated high P-wave velocity layers at depths of 15−30 km, which are possibly related to the crystalline mafic rocks or high-grade metamorphic rocks associated with mantle-derived magmas [43].

Meanwhile, partial melting also contributes to modifying the existing mineral deposits in the Tanlu Fault [42]. With the deep subduction of the Yangtze Craton and the continuous compression of the subducted Pacific Plate [43], partially melted rocks and high fluid can develop regularly seismic anomalies and spaced melt channels along the deep faults at high temperatures and pressures [44,45]. These melt channels allow flow and movement between different scale lenses of rocks (10−20 m). The key feature of the Tanlu Fault is the presence of high-temperature, low-pressure metamorphic rocks, such as granulites and migmatites [46]. These rocks are thought to have formed due to the partial melting of the lower crust and the deep subduction of the Yangtze Craton and Paleo-Pacific subduction. The deep subduction process also created high temperatures and pressures that led to the formation of granitic rocks in the Tanlu Fault. The granitic rocks then interacted with the surrounding rocks to form mineral deposits, such as tungsten, tin, and molybdenum (Fig. 2) [46,47].

Combined with the geophysical results and the geological data, a new model is proposed for the mafic intrusion model associated with partial melting (Fig. 10). The model indicates that mafic intrusions are composed of dense, iron- and magnesium-rich rocks, such as basalt or gabbro, which can cause significantly high seismic wave velocities in the middle and lower crust [47]. The intrusion possibly has been emplaced through the Tanlu Fault and other deep large faults during an episode of magma emplacement in the region [47].

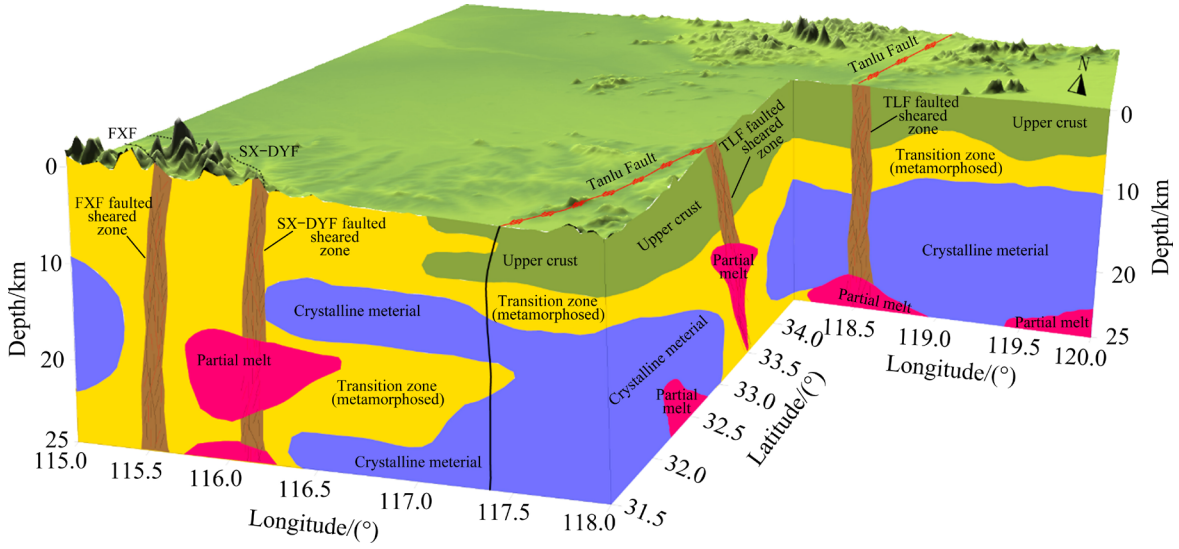

Fig. 10 3D mafic intrusion model associated with partial melting

6 Conclusions

(1) The prominent low-velocity anomalies are distributed extensively along the Tanlu and Feixi Faults, extending into the middle and lower crust, which are accompanied by a significant concentration of seismic activity, indicating that the two faults are deep and extensive fault zones.

(2) Due to the deep subduction of the Yangtze Craton and the continuous compression of the subducted Pacific Plate, partially melted rocks and high fluid are widely developed and new metamorphic minerals are formed, which cause regular seismic anomalies and space melt channels along the deep faults. These fault zones serve as conduits for magma intrusion.

(3) Combined with the distribution of HP/UHP metamorphic rocks and seismic velocity anomaly in the Dabie Orogenic Belt, a two-stage formation model is built for HP/UHP metamorphic rocks controlled by buoyancy and corner flow in the Dabie Orogenic Belt.

CRediT authorship contribution statement

Ya SUN: Project administration, Funding acquisition, Formal analysis, Writing − Review and editing; **Zi-jun YUAN:** Investigation, Validation, Visualization, Writing − Original draft; **Ji-wen HUANG:** Formal analysis, Writing − Review and editing; **Jian-tai ZHANG** and **Fu-quan LI:** Supervision, Data curation; **Jian-xin LIU:** Writing − Review and editing.

Declaration of competing interest

The authors declare that they have no known competing financial interests or personal relationships that could have appeared to influence the work reported in this paper.

Acknowledgments

The study was supported by the National Natural Science Foundation of China (Nos. 42574119, 42274083, 41974049) and partly supported by the Urban Geological Survey Project of Linyi, Shandong Province, China (No. SDGP371300202102000468).

References

[1] HUANG Lei, LIU Chi-yang, KUSKY T M. Cenozoic evolution of the Tanlu Fault zone (East China)—Constraints from seismic data [J]. Gondwana Research, 2015, 28(3): 1079−1095.

[2] SU Zhe, XU Xi-wei, LIANG Shan-shan, WANG E. Seismotectonics of the 2017—2018 Songyuan earthquake sequence, Northeastern China: Passive bookshelf faulting and block rotation in the Songliao Basin [J]. Seismological Research Letters, 2020, 91(3): 1593−1605.

[3] LIN Ai-ming, TAKAO M, WAN Tian-feng. Tectonic characteristics of the central segment of the Tancheng–Lujiang Fault zone, Shandong Peninsula, Eastern China [J]. Tectonophysics, 1998, 293(1/2): 85−104.

[4] CHEN Yuan-lin, LI Huan, ZHENG Chao-yang, LI Da-dou. Denudation degree and deep prospecting potential of gold deposits in Guocheng—Yazi Fault zone, Jiaolai basin [J]. The Chinese Journal of Nonferrous Metals, 2022, 32(9): 2819−2834.

[5] WANG Yue-jun, FAN Wei-ming, ZHANG Guo-wei, ZHANG Yan-hua. Phanerozoic tectonics of the South China Block: Key observations and controversies [J]. Gondwana Research, 2013, 23(4): 1273−1305.

[6] CHEN L, ZHENG T, XU W W. A thinned lithospheric image of the Tanlu Fault Zone, eastern China: Constructed from wave equation-based receiver function migration [J]. Journal of Geophysical Research: Solid Earth, 2006, 111: B09312.

[7] LIU Xin, ZHAO Da-peng, LI San-zhong, WEI Wei. Age of the subducting Pacific slab beneath East Asia and its geodynamic implications [J]. Earth and Planetary Science Letters, 2017, 464: 166−174.

[8] LEI Jian-she, ZHAO Da-peng, XU Xi-wei, DU Mo-fei, MI Qi, LU Ming-wen. P-wave upper-mantle tomography of the Tanlu Fault zone in Eastern China [J]. Physics of the Earth and Planetary Interiors, 2020, 299: 106402.

[9] LI C L, CHEN C X, DONG D D, KUPONIYI A P, DOSSO S E, SU D L. Ambient noise tomography of the Shandong province and its implication for Cenozoic intraplate volcanism in Eastern China [J]. Geochemistry, Geophysics, Geosystems, 2018, 19(9): 3286−3301.

[10] MA Li-xue, XU Tao, AI Yin-shuang, YANG Jin-hui, YANG Ying-jie, FAN En-bo, LI Long, HOU Jue, DONG Wei-yu. Hot lithosphere beneath the northeastern North China Craton detected by ambient noise tomography [J]. Tectonophysics, 2022, 839: 229551.

[11] SHI Da-nian, LÜ Qing-tian, XU Wen-yi, YAN Jia-yong, ZHAO Jin-hua, DONG Shu-wen, CHANG Yin-fo. Crustal structure beneath the middle–lower Yangtze metallogenic belt in East China: Constraints from passive source seismic experiment on the Mesozoic intra-continental mineralization [J]. Tectonophysics, 2013, 606: 48−59.

[12] GU Qin-ping, LI Da-hu, DING Zhi-feng, KANG Qing-qing, YU Yue-ying, WANG Jun-fei, MENG Ke, YANG Hao, ZHANG Hao, LÜ Yun-fu. Crustal structure characteristics beneath the Shandong−Jiangsu−Anhui segment of the Tanlu Fault zone and its adjacent regions using receiver functions [J]. Chinese Journal of Geophysics, 2022, 65(9): 3280−3296.

[13] SHAHZAD M S, LIU Jian-xin, SUN Ya, LI Chuan. Crustal structure and deformation in southeastern China revealed by receiver functions [J]. Journal of Asian Earth Sciences, 2021, 221: 104937.

[14] TIAN Fan-fan, LEI Jian-she, XU Xi-wei. Teleseismic P-wave crustal tomography of the Weifang segment on the Tanlu Fault zone: A case study based on short-period dense seismic array experiment [J]. Physics of the Earth and Planetary Interiors, 2020, 306: 106521.

[15] LI Xiao-yong, ZHU Pei-min, KUSKY T M, GU Yuan, PENG Song-bai, YUAN Yue-feng, FU Jian-min. Has the Yangtze craton lost its root? A comparison between the North China and Yangtze cratons [J]. Tectonophysics, 2015, 655: 1−14.

[16] SUN Ya, DENG Shi-lin, LIU Jian-xin, SHAZAD S M, CHEN Bo. Hydrothermal activity and metallogenic environment revealed by seismic wave tomography in Yunnan Province, China [J]. Transactions of Nonferrous Metals Society of China, 2023, 33(11): 3476−3486.

[17] KANG Yue-lan, SHI Yu-ruo, ANDERSON J L, YANG Tian-shui, ZHANG Hai-jun. Mesozoic tectono-magmatic evolution of the Tanlu Fault zone and its relationship with the destruction of the North China Craton [J]. International Geology Review, 2024, 66(11): 2001−2030.

[18] JIANG Guo-ming, ZHANG Gui-bin, ZHAO Da-peng, LÜ Qing-tian, LI Hong-yi, LI Xin-fu. Mantle dynamics and Cretaceous magmatism in east-central China: Insight from teleseismic tomograms [J]. Tectonophysics, 2015, 664: 256−268.

[19] WU Yuan-bao, ZHENG Yong-fei. Tectonic evolution of a composite collision orogen: An overview on the Qinling—Tongbai—Hong'an—Dabie—Sulu orogenic belt in Central China [J]. Gondwana Research, 2013, 23(4): 1402−1428.

[20] LIU Jian-xin, SHAHZAD M S, SUN Y, SHAHZAD A, LI Chuan, FANIDI M, MUHAMMAD I. Deep metallogenic mechanism in southeastern China based on receiver function data [J]. Transactions of Nonferrous Metals Society of China, 2022, 32(1): 273−284.

[21] ZHANG Kai-jun, CAI Jian-xin, ZHU Jun-xing. North China and South China collision: Insights from analogue modeling [J]. Journal of Geodynamics, 2006, 42(1/2/3): 38−51.

[22] SHEN Wei-sen, RITZWOLLER M H, KANG Dou, KIM Y H, LIN Fan-chi, NING Jie-yuan, WANG Wei-tao, ZHENG Yong, ZHOU Long-quan. A seismic reference model for the crust and uppermost mantle beneath China from surface wave dispersion [J]. Geophysical Journal International, 2016, 206(2): 954−979.

[23] WANG Qiang, WYMAN D A, XU Ji-feng, ZHAO Zhen-hua, JIAN Ping, XIONG Xiao-lin, BAI Zheng-hua. Petrogenesis of Cretaceous adakitic and shoshonitic igneous rocks in the Luzong area, Anhui Province (Eastern China): Implications for geodynamics and Cu–Au mineralization [J]. Lithos, 2006, 89(3/4):424−446.

[24] SONG Shi-wei, MAO Jing-wen, ZHU Yong-feng, YAO Zai-yu, CHEN Guo-hua, RAO Jian-feng, OUYANG Yong-peng. Partial-melting of fertile metasedimentary rocks controlling the ore formation in the Jiangnan porphyry-skarn tungsten belt, South China: A case study at the giant Zhuxi W−Cu skarn deposit [J]. Lithos, 2018, 304: 180−199.

[25] ZHANG Hai-jiang, THURBER C H. Development and applications of double-difference seismic tomography [J]. Pure and Applied Geophysics, 2006, 163: 373−403.

[26] ZHANG Hai-jiang, THURBER C H. Double-difference tomography: The method and its application to the Hayward fault, California [J]. Bulletin of the Seismological Society of America, 2003, 93(5): 1875−1889.

[27] WALDHAUSER F, ELLSWORTH W L. A double-difference earthquake location algorithm: Method and application to the northern Hayward Fault, California [J]. Bulletin of the Seismological Society of America, 2000, 90(6): 1353−1368.

[28] BROCHER T M. Empirical relations between elastic wave speeds and density in the Earth's crust [J]. Bulletin of the Seismological Society of America, 2005, 95(6): 2081−2092.

[29] LUO Yin-he, XU Yi-xian, YANG Ying-jie. Crustal structure beneath the Dabie orogenic belt from ambient noise tomography [J]. Earth and Planetary Science Letters, 2012, 313: 12−22.

[30] WANG Chun-yong, ZENG Rong-sheng, MOONEY W D, HACKER B R. A crustal model of the ultrahigh-pressure Dabie Shan orogenic belt, China, derived from deep seismic refraction profiling [J]. Journal of Geophysical Research: Solid Earth, 2000, 105: 10857−10869.

[31] JI Shao-cheng, WANG Qian, MARCOTTE D, SALISBURY M H, XU Zhi-qin. P wave velocities, anisotropy and hysteresis in ultrahigh-pressure metamorphic rocks as a function of confining pressure [J]. Journal of Geophysical Research: Solid Earth 2007, 112: B09204.

[32] WU Yao, FEI Ying-wei, JIN Zhen-min, LIU Xiao-yang. The fate of subducted upper continental crust: An experimental study [J]. Earth and Planetary Science Letters, 2009, 282(1/2/3/4): 275−284.
[33] WANG Qing-chen, SHI Yong-hong, LIN Wei, GUO Jing-hui. Exhumation of the Dabie UHP terrane, China [J]. International Geology Review, 2008, 50(1): 15−31.
[34] LIU Fu-tian, XU Pei-fen, CHUN Kin-yi, LIU song, YIN Zhou-xun. Crustal velocity structure of the deep continental subduction zone—A wide angle reflection/refraction seismic study on the eastern dabie orogeny [J]. Chinese Journal of Geophysics, 2003, 46(3): 526−534.
[35] ZOU Zhi-hui, ZHOU Hua-wei, LIN Fan-sheng, FANG Li-hua, LI San-zhong. High-resolution teleseismic tomographic crustal imaging for potential seismogenic segment of the central Tanlu Fault zone, East China [J]. Tectonophysics, 2022, 823: 229196.
[36] BEM T S, YAO Hua-jian, LUO Song, YANG Yuan, WANG Xing-zhou, WANG Xiao-li, LI Ling-li, LIU Bin. High-resolution 3-D crustal shear-wave velocity model reveals structural and seismicity segmentation of the central-southern Tanlu Fault Zone, Eastern China [J]. Tectonophysics, 2020, 778: 228372.
[37] MENG Ya-feng, YAO Hua-jian, WANG Xin-zhou, LI Ling-li, FENG Ji-kun, HONG De-quan, WANG Xiao-li. Crustal velocity structure and deformation features in the central−southern segment of Tanlu Fault zone and its adjacent area from ambient noise tomography [J]. Chinese Journal of Geophysics, 2019, 62(7): 2490−2509.
[38] LÜ Zi-qiang, LEI Jian-she. Seismic evidence for crustal modification across the Tanlu Fault zone in Eastern China [J]. Geophysical Research Letters, 2022, 49(17): e2022GL099761.
[39] LI Ling-li, SHEN Wei-sen, SUI Si-yuan, YAO Hua-jian, BAO Zi-wen. Crustal thickness beneath the Tanlu Fault zone and its tectonic significance based on two-layer H−κ stacking [J]. Earthquake Science, 2021, 34(1): 47−63.
[40] MOTRA H B, STUTZ H H. Geomechanical rock properties using pressure and temperature dependence of elastic P- and S-wave velocities [J]. Geotechnical and Geological Engineering, 2018, 36: 3751−3766.
[41] JOHNSON S E, SONG W J, COOK A C, VEL S S, GERBI C C. The quartz α–β phase transition: Does it drive damage and reaction in continental crust? [J]. Earth and Planetary Science Letters, 2021, 553: 116622.
[42] WANG Lu, KUSKY T M, POLAT A, WANG Song-jie, JIANG Xing-fu, ZONG Ke-qing, FU Jian-min. Partial melting of deeply subducted eclogite from the Sulu orogen in China [J]. Nature Communications, 2014, 5(1): 5604.
[43] JAHN B M, WU F Y, LO C H, TSAI C H. Crust–mantle interaction induced by deep subduction of the continental crust: Geochemical and Sr–Nd isotopic evidence from post-collisional mafic–ultramafic intrusions of the northern Dabie complex, central China [J]. Chemical Geology, 1999, 157(1/2): 119−146.
[44] ZHAO Yi, ZHENG Jian-ping, XIONG Qing, ZHANG Hui. Destruction of the North China Craton triggered by the Triassic Yangtze continental subduction/collision: A review [J]. Journal of Asian Earth Sciences, 2018, 164: 72−82.
[45] GAO S, RUDNICK R L, XU W L, YUAN H L, LIU Y S, WALKER R J, PUCHTEL I S, LIU X M, HUANG H, WANG X R, YANG J. Recycling deep cratonic lithosphere and generation of intraplate magmatism in the North China Craton [J]. Earth and Planetary Science Letters, 2008, 270(1/2): 41−53.
[46] TAN Jun, WEI Jun-hao, GUO Ling-li, ZHANG Ke-ping, YAO Chun-liang, LU Jian-pei. LI Hong-mei. LA−ICP−MS zircon U-Pb dating and phenocryst EPMA of dikes, Guocheng, Jiaodong Peninsula: Implications for North China Craton lithosphere evolution [J]. Science in China Series D: Earth Sciences, 2008, 51(10): 1483−1500.
[47] PALIN R M, WHITE R W, GREEN E C R. Partial melting of metabasic rocks and the generation of tonalitic–trondhjemitic–granodioritic (TTG) crust in the Archaean: Constraints from phase equilibrium modelling [J]. Precambrian Research, 2016, 287: 73−90.

P 波成像揭示郯庐断裂带中南段的成矿环境

孙 娅[1]，袁子君[1]，黄基文[1]，张建太[2]，李付全[2]，柳建新[1]

1. 中南大学 地球科学与信息物理学院，长沙 410083；
2. 山东省地质矿产勘查开发局第七地质大队，临沂 276000

摘 要：利用双差层析成像技术构建了郯庐断裂带中南段 P 波速度模型。研究结果显示，在郯庐断裂带和肥西断裂带周围存在从地表向下延伸到地壳下深度为 25 km 的低速异常，这是由于断层附近物质部分熔融产生的流体引起的。地震重新定位结果表明，在郯庐和肥西断裂带周围 20 km 以上的地震活动明显集中，表明深大断裂带可能是深部矿物向上迁移的通道。结合地质和地球物理数据，所提出的地质动力学模型揭示，深部矿化物质的迁移沿着郯庐断裂带延伸。所得结果为阐明郯庐断裂带中南段复杂的成矿过程提供了重要基础，从而加深了人们对矿体形成、断层流体、局部熔融和地震活动之间相互作用的理解。

关键词：郯庐断裂带中南段；双差层析成像；矿化；局部熔融；P 波速度

(Edited by Wei-ping CHEN)